A Graph Theoretic Approach to Dynamic Functional Connectivity Tracking and Network State Identification

David M. Zoltowski[1], Edward M. Bernat[2] and Selin Aviyente[1]

Abstract— **With the advances in neuroimaging technology, it is now possible to measure human brain activity with increasing temporal and spatial resolution. This vast amount of spatio-temporal data requires the development of computational methods capable of building an integrated picture of the functional networks for a better understanding of the healthy and diseased brain [1]. Although the construction of these networks from neuroimaging data is well-established [2], current approaches are limited to the characterization of the global topology of static networks where the links between different brain regions represent average connectivity over a long time period [3], [2]. Recent studies suggest that human cognition arises from the rapid formation and dissociation of synchronized neural activity on short time scales in the order of milliseconds [4]. There is a strong need for new electroencephalogram (EEG)-based analytic frameworks for monitoring dynamic functional network activity. In this paper, we propose a graph theoretic approach for tracking the changing topology of functional connectivity networks across time. First, we introduce an event detection algorithm based on node level feature extraction and principal components analysis of time-dependent node correlation matrices. Then, we propose a k-means based clustering approach to characterize each time interval with the most common connectivity states. Finally, the proposed methodology is applied to the study of the dynamics of functional connectivity networks during error-related negativity (ERN).**

I. INTRODUCTION

With the advance in noninvasive imaging modalities, there is growing evidence that human cognition arises from the integration of neural activity from functionally distinct neurocognitive networks, known as functional connectivity (FC). Most of the current work is based on the assumption that functional connectivity is stationary both temporally and spatially. However, empirical evidence along with experimental neuroimaging studies have recently revealed that the functional connectivity fluctuates across time across multiple scales [5].

Recently, a few studies focused on the evolution of connectivity patterns and network metrics estimated from multichannel neurophysiological recordings [6], [7], [8]. The early papers in this area use a moving time-window to construct time-varying functional connectivity graphs (FCGs) from multichannel neurophysiological recordings [6], [7], and employ topographical graph measures to summarize the evolution of these networks across time and within a frequency band. However, these methods have a couple of drawbacks. By computing a topological measure for each FCG, these methods cannot capture the spatial variations and thus are unable to determine the network components that contribute to the change in organization. The more recent research in the area of time-varying FCGs attempts to address these issues by developing a framework for extracting functional connectivity microstates (FCμstates) or network states defined as short lasting quasi-stationary connectivity patterns [5], [8]. In [5], temporally invariant network states were defined by first representing each FCG as a vector, constructing a similarity matrix in time between all FCGs, and clustering to identify the temporal boundaries of each network state. Series of temporally adjacent networks assigned to the same cluster comprised a coherent network state summarized by the average of FCGs in that time interval.

In this paper, we contribute to this line of work and offer some improvements. First, unlike current work which mostly relies on the raw functional connectivity graphs at each time point, we offer a feature based similarity approach to track the network dynamics in time. Well-known graph theoretic measures for weighted graphs are used to extract node level features at each time point. Next, correlation matrices across sliding time windows are constructed to quantify the similarity between the different nodes in the network. The principal eigenvector of these correlation matrices are then used to detect the transition points between different network states. This approach offers a way of directly correlating the nodes and identifying change points based on changes in the nodes' attributes. Once these transition points are identified, a collection of representative network topographies are extracted for each interval across multiple subjects through k-means clustering, unlike current methods which usually consider the average connectivity to summarize network states. Finally, the proposed framework is applied to the study of error related negativity in the brain across multiple subjects.

II. BACKGROUND

In this section, we will review the basics of functional connectivity measures, in particular the time-varying phase synchrony measure, and some common graph theoretic measures for weighted graphs.

A. Time-Varying Functional Networks

The time-varying functional brain networks are generated where the nodes of the graphs correspond to different

This work was in part supported by the National Science Foundation under Grant No. CCF-1218377.

[1] D. M. Zoltowski and S. Aviyente are with the Department of Electrical and Computer Engineering, Michigan State University, East Lansing, MI 48824, USA. Emails: zoltow11@msu.edu, aviyente@egr.msu.edu.

[2]E. Bernat is with the Department of Psychology, University of Maryland, College Park, MD 20742, USA. Email: edward.m.bernat@gmail.com.

brain regions and the edges correspond to the connectivity strengths. In this paper, we quantify the connectivity using a recent phase synchrony measure based on RID-Rihaczek distribution [9]. This measure has been shown to be more robust to noise and to provide better resolution as discussed in [9].

First, we quantify the time-varying phase of a signal, $\Phi_i(t,\omega) = \arg\left[\frac{C_i(t,\omega)}{|C_i(t,\omega)|}\right]$ where $C_i(t,\omega)$ is the complex RID-Rihaczek distribution[1]:

$$C_i(t,\omega) = \int\int \underbrace{\exp\left(-\frac{(\theta\tau)^2}{\sigma}\right)}_{\text{Choi-Williams kernel}} \underbrace{\exp(j\frac{\theta\tau}{2})}_{\text{Rihaczek kernel}} A_i(\theta,\tau)e^{-j(\theta t+\tau\omega)}d\tau d\theta \tag{1}$$

and $A_i(\theta,\tau) = \int s_i(u+\frac{\tau}{2})s_i^*(u-\frac{\tau}{2})e^{j\theta u}du$ is the ambiguity function of $\boldsymbol{s}_i$. The phase synchrony between nodes i and j at time t and frequency ω is computed using 'Phase Locking Value' (PLV):

$$PLV_{i,j}(t,\omega) = \frac{1}{L}\left|\sum_{k=1}^{L}\exp\left(j\Phi_{i,j}^k(t,\omega)\right)\right| \tag{2}$$

where L is the number of trials and $\Phi_{i,j}^k(t,\omega) = |\Phi_i(t,\omega) - \Phi_j(t,\omega)|$ is the phase difference estimate between the two nodes for the k^{th} trial.

Let $\{\boldsymbol{G}(t)\}_{t=1,2,\ldots,T}$ be a time sequence of graphs where $\boldsymbol{G}(t)$ is an $N \times N$ weighted and undirected graph corresponding to the functional connectivity network at time t for a fixed frequency or frequency band, T is the total number of time points and N is the number of nodes within the network. The time-varying edge values are quantified by the average PLV within a frequency band and at a certain time as:

$$G_{i,j}(t) = \frac{1}{\Omega}\sum_{\omega=\omega_a}^{\omega_b} PLV_{i,j}(t,\omega) \tag{3}$$

where $G_{i,j}(t) \in [0,1]$ represents the connectivity strength between the nodes i and j within the frequency band of interest, $[\omega_a,\omega_b]$, and Ω is the number of frequency bins in that band.

B. Graph Theoretic Measures

Recent developments in the quantitative analysis of complex networks, based largely on graph theory, have been rapidly translated to studies of brain network organization [2]. In this paper, we will apply graph theoretic topological measures defined particularly for weighted networks to extract features from each node. In particular, we will focus on the clustering coefficient, path length and centrality measures. For a node n, the weighted local clustering coefficient C_n is defined as

$$C_n = \frac{2t_n^w}{k_n(k_n-1)}, \tag{4}$$

[1]The details of the RID-Rihaczek distribution and the corresponding synchrony measure are given in [9].

where t_n^w is the weighted geometric mean of triangles around node n and k_n is the weighted degree of node n [3]. The average shortest path length L_n of a node n is

$$L_n = \frac{1}{N}\sum_{j=1}^{N} D_{nj}, \tag{5}$$

where D_{jk} is the shortest path distance, computed as the sum of the edge weights, between nodes j and k. Lastly, the eigenvector centrality E_n is computed by selecting the n^{th} element of the principal eigenvector $\mathbf{e}$ of a graph $\mathbf{G}$ such that

$$E_n = \frac{1}{\lambda}\sum_{j=1}^{N}\mathbf{G}_{nj}e_j, \tag{6}$$

where λ is a constant [3], [10].

III. Methods

A. Event Interval Identification

Since the connectivity networks are fully connected, we first identified significant edges of the networks using Dijkstra's algorithm [11]. Let $\mathbf{G}^s(t)$ be the weighted graphs produced by Dijkstra's algorithm, where $s = 1,2,\ldots,S$, $t = 1,2,\ldots,T$, S is the number of subjects, and T is the number of time points. Node level features were extracted from the weighted graphs composed of the significant edges. For a given time point t and subject s, three features were extracted from the N nodes of graph $\mathbf{G}^s(t)$ into a feature vector $\mathbf{f}_i^s(t) \in \mathbb{R}^{N\times 1}$, where $i = 1,2,3$. For a node n at time t for subject s, $\mathbf{f}_1^s(t)(n) = C_n$, $\mathbf{f}_2^s(t)(n) = L_n$, and $\mathbf{f}_3^s(t)(n) = E_n$. For each feature i, we constructed the tensor $\mathcal{X}^i \in \mathbb{R}^{T\times N\times S}$, where $\mathcal{X}^i(t,n,s) = \mathbf{f}_i^s(t)(n)$.

Our goal was to capture the time-varying changes in the networks across all subjects. We used Tucker decomposition to compress each tensor along the subject mode. The full Tucker decomposition [12] of $\mathcal{X}$ is

$$\mathcal{X} = \mathcal{C}\times_1\mathbf{U}_1\times_2\mathbf{U}_2\times_3\mathbf{U}_3 \tag{7}$$

where $\mathcal{C}$ is a core tensor with the same dimensions as $\mathcal{X}$, $\times_k$ is the multiplication of a tensor with a matrix along the k^{th} mode, and $\mathbf{U}_k \in \mathbb{R}^{I\times I}$ is a component matrix for the k^{th}-mode, where I is the size of $\mathcal{X}$ along mode k. The Frobenius-norms of the subtensors $\mathbf{C}_{k=j}$ obtained by fixing the k^{th} dimension decrease in value as j is increased [13] and are singular values of the tensor along the i^{th} mode. An elbow criterion was used to select the optimal number of singular values. The original tensor was compressed along the subject mode by projecting the tensor onto the corresponding singular vectors. That is, for tensor $\mathcal{X}^i \in \mathbb{R}^{t\times n\times s}$ corresponding to feature i, we have a matrix $\hat{\mathbf{X}}^i$

$$\hat{\mathbf{X}}^i = \sum_{m=1}^{M} w_m\ \mathcal{X}^i\times_3\mathbf{U}_3^m \tag{8}$$

where $w_m = \frac{\|\mathbf{C}_{3=m}\|_F}{\sum_{s=1}^{S}\|\mathbf{C}_{3=s}\|_F}$ and $\mathbf{U}_3^m$ is the m^{th} column of $\mathbf{U}_3$.

In order to capture the variation in the node activity over time, we computed correlation matrices over time using a

sliding window. For each time window with length W and feature i we calculated a correlation matrix $\mathbf{C}^i_{jk}$

$$\mathbf{C}^i_{jk}(t) = |\rho(\hat{\mathbf{X}}^i([t-W+1,t],j), \hat{\mathbf{X}}^i([t-W+1,t],k))| \quad (9)$$

where ρ is the correlation function and $\mathbf{C}^i_{jk}$ is the absolute value of the correlation between the values of the feature i at nodes j and k over the time window. Next, for a feature i, we compared the principal eigenvector $\mathbf{u}^i(t)$ of each correlation matrix with the average of $\hat{W}$ past principal eigenvectors $\mathbf{v}^i(t) = \frac{1}{\hat{W}} \sum_{k=t-\hat{W}}^{t-1} \mathbf{u}^i(k)$.

Events of interest were identified by computing similarity between the principal eigenvector $\mathbf{u}^i(t)$ at the current time point with typical behavior, i.e. $\mathbf{v}^i(t)$, using a cosine similarity measure. The angle between the two vectors is computed as:

$$\theta^i(t) = \arccos\left(\frac{\langle \mathbf{u}^i(t), \mathbf{v}^i(t)\rangle}{\|\mathbf{u}^i(t)\|_2 \|\mathbf{v}^i(t)\|_2}\right), \quad (10)$$

where $\langle \cdot, \cdot \rangle$ is the inner product operator.

The angles $\theta^i(t)$ indicate how the current time point t differs from the previous $\hat{W}$ time points for a feature i. We averaged the angles for the different features to compute a z-score $\mathbf{z}(t)$ at each t

$$\mathbf{z}(t) = 1 - \cos\left(\frac{1}{3}\sum_{i=1}^{3} \theta^i(t)\right). \quad (11)$$

When the z-score of a time point t was larger than two standard deviations from the mean of $\mathbf{z}(t)$, we detected that time point as a change point.

B. Network State Characterization

Once the different time intervals were identified, for each time interval $[T1, T2]$ we cluster the collection of connectivity matrices

$$\{\mathbf{G}^1(T1), \ldots, \mathbf{G}^1(T2), \mathbf{G}^2(T1), \ldots \mathbf{G}^2(T2), \mathbf{G}^S(T1), \ldots \mathbf{G}^S(T2)\}$$

using the k-means algorithm. The clustering was initiated with random seed, the distance measure was the ℓ_2 norm, and the clustering was replicated 250 times. The number of clusters was chosen to maximize the Fisher score

$$F = \mathrm{tr}\{(\mathbf{S}_b)(\mathbf{S}_t + \gamma \mathbf{I})^{-1}\} \quad (12)$$

where $\mathbf{S}_b$ and $\mathbf{S}_t$ are the between-class scatter matrix and total scatter matrix, respectively [14].

IV. Results

A. EEG Data

The proposed framework is applied to a set of EEG data containing the error-related negativity (ERN). The ERN is a brain potential response that occurs following performance errors in a speeded reaction time task usually 25-75 ms after the response [15]. Previous work [16] indicates that there is increased coordination between the lateral prefrontal cortex (lPFC) and medial prefrontal cortex (mPFC) within the theta frequency band (4-8 Hz) and ERN time window (25- 75 ms), supporting the idea that frontal and central electrodes are functionally integrated during error processing. EEG data from 63-channels with a sampling rate of 128 Hz was collected in accordance with the 10/20 system on a Neuroscan Synamps2 system (Neuroscan, Inc.). A speeded-response flanker task was employed, and response-locked averages were computed for each subject. All EEG epochs were converted to current source density (CSD) using published methods [17]. In this paper, we analyzed data from 91 subjects corresponding to the error responses.

B. Event Intervals

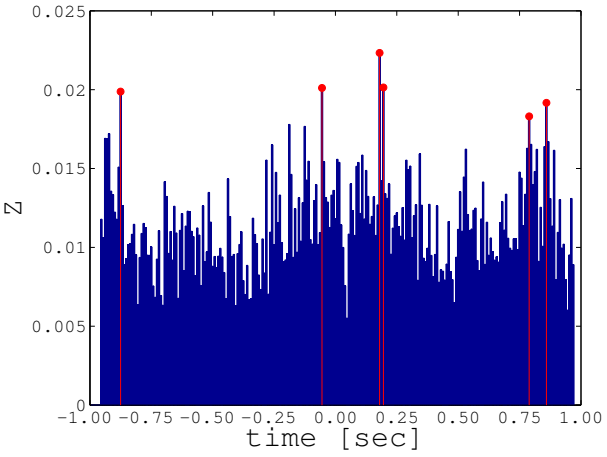

Fig. 1. The Z-scores corresponding to the combination of the local clustering coefficient, average shortest path length, and eigenvector centrality measures, for a window length of 5 samples. The points in red denote change points that are greater than two standard deviations from the mean Z-score.

In our analysis, we first constructed time-varying graphs with $N = 63$, $T = 256$, and $S = 91$ where the edge values were the average PLV over the frequency band [2,7] Hz. From each graph, we extracted three features and for each feature formed the tensor $\mathcal{X}^i \in \mathbb{R}^{63\times256\times91}$. We chose $W = 5$ corresponding to 39.0625 ms. The z-score was computed by comparing the current principal vector with the average of the past 5 principal vectors. The combined z-score across time is shown in Fig. 1. Based on this figure, we detected 6 change points. Two of the change points, specifically the two near the 0.25 second mark, are 2 samples apart, which is smaller than our window; therefore, we decided to consolidate those points into one change point. From this analysis, we determined six event intervals: $[-1000, -875.0)$, $[-875.0, -54.7)$, $[-54.7, 187.5)$, $[187.5, 789.1)$, $[789.1, 859.4)$, and $[859.4, 1000)$ ms. It is important to note that $[-54.7, 187.5)$ corresponds to the ERN time window and $[187.5, 789.1)$ corresponds to the P3e interval.

C. Topographic Distribution of Network States

For each time interval, we clustered the connectivity matrices into two clusters using k-means, where the number of clusters was chosen to maximize the Fisher score. In order to highlight the changes between the different time intervals,

in Fig. 2 we plot the centroid representing the first time interval and the differences between the following centroids and this initial one.

In the pre-response interval shown in Fig. 2-a there is no localized activity. Then, during the interval shown in Fig. 2-b, more focal activity emerges that involves separable connections within frontal and parietal-occipital regions. This is consistent with ongoing stimulus processing in occipital and parietal regions combined with prefrontal engagement to guide responding. During the ERN interval in Fig. 2-c, most broad activity is suppressed, particularly for frontal regions, and only a narrow lateral-central connection frontally appears to maintain a strong connection. Next, in Fig. 2-d, the network suppression begins to lessen and frontal and parietal connections begin to reemerge. Finally, in Fig. 2-e, suppression appears to be over, and broad frontal and parietal connectivity returns.

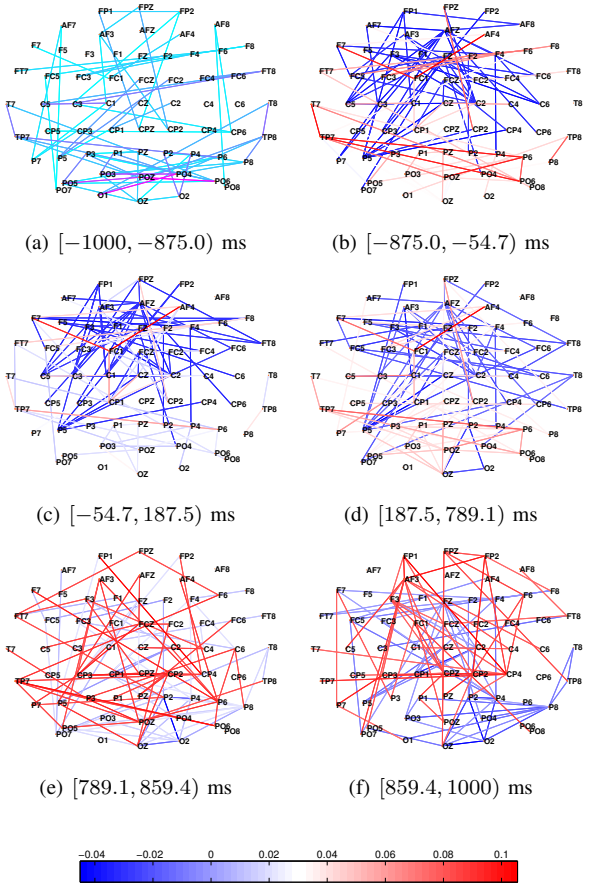

Fig. 2. (a) Topographical map of the top 5% of the significant connections in the centroid with the highest membership for the first time interval. (b)-(f) The top 2.5% largest magnitudes of both the positive (red) and negative (blue) differences between the centroids for the given time interval and the first time interval.

V. CONCLUSIONS

In this paper, we introduced a graph theoretic approach to identify event intervals and characterize network states for dynamic functional connectivity networks. We characterized the connectivity graphs in terms of their node features and use a Tucker decomposition to capture subject variation in the node-feature space. Change-points are detected by comparing the principal eigenvectors of current time points with recent past time points. Network states are then determined by clustering the connectivity matrices. The centroids of the resulting clusters indicate the network states for each interval and differences in the centroids highlight changes between different time intervals. Future work will concentrate on how to better distinguish the background or default mode network of the brain from the network connections that are simply due to the response and cognitive processes.

REFERENCES

[1] B. He, T. Coleman, G. M. Genin, G. Glover, X. Hu, N. Johnson, T. Liu, S. Makeig, P. Sajda, and K. Ye, "Grand challenges in mapping the human brain: Nsf workshop report," *IEEE transactions on biomedical engineering*, vol. 60, no. 11, pp. 2983–2992, 2013.

[2] E. Bullmore and O. Sporns, "Complex brain networks: graph theoretical analysis of structural and functional systems," *Nature Reviews Neuroscience*, vol. 10, no. 3, pp. 186–198, 2009.

[3] M. Rubinov and O. Sporns, "Complex network measures of brain connectivity: uses and interpretations," *Neuroimage*, vol. 52, no. 3, pp. 1059–1069, 2010.

[4] D. Bassett, N. Wymbs, M. Porter, P. Mucha, J. Carlson, and S. Grafton, "Dynamic reconfiguration of human brain networks during learning," *Proceedings of the National Academy of Sciences*, vol. 108, no. 18, pp. 7641–7646, 2011.

[5] R. F. Betzel, M. A. Erickson, M. Abell, B. F. O'Donnell, W. P. Hetrick, and O. Sporns, "Synchronization dynamics and evidence for a repertoire of network states in resting eeg," *Frontiers in computational neuroscience*, vol. 6, 2012.

[6] S. Dimitriadis, N. Laskaris, V. Tsirka, M. Vourkas, S. Micheloyannis, and S. Fotopoulos, "Tracking brain dynamics via time-dependent network analysis," *Journal of Neuroscience Methods*, vol. 193, no. 1, pp. 145–155, 2010.

[7] M. Valencia, J. Martinerie, S. Dupont, and M. Chavez, "Dynamic small-world behavior in functional brain networks unveiled by an event-related networks approach," *Physical Review E*, vol. 77, no. 5, p. 050905, 2008.

[8] S. Dimitriadis, N. Laskaris, and A. Tzelepi, "On the quantization of time-varying phase synchrony patterns into distinct functional connectivity microstates (fcμstates) in a multi-trial visual erp paradigm," *Brain topography*, vol. 26, no. 3, pp. 397–409, 2013.

[9] S. Aviyente and A. Mutlu, "A time-frequency-based approach to phase and phase synchrony estimation," *IEEE Transactions on Signal Processing*, vol. 59, no. 7, pp. 3086–3098, 2011.

[10] M. E. Newman, "Analysis of weighted networks," *Physical Review E*, vol. 70, no. 5, p. 056131, 2004.

[11] E. Dijkstra, "A note on two problems in connexion with graphs," *Numerische Mathematik*, vol. 1, no. 1, pp. 269–271, 1959. [Online]. Available: http://dx.doi.org/10.1007/BF01386390

[12] T. G. Kolda and B. W. Bader, "Tensor decompositions and applications," *SIAM review*, vol. 51, no. 3, pp. 455–500, 2009.

[13] L. De Lathauwer, B. De Moor, and J. Vandewalle, "A multilinear singular value decomposition," *SIAM journal on Matrix Analysis and Applications*, vol. 21, no. 4, pp. 1253–1278, 2000.

[14] Q. Gu, Z. Li, and J. Han, "Generalized fisher score for feature selection," *Proc. Conf. Uncertainty in Artificial Intelligence*, pp. 266–273, 2011.

[15] J. R. Hall, E. M. Bernat, and C. J. Patrick, "Externalizing psychopathology and the error-related negativity," *Psychological Science*, vol. 18, no. 4, pp. 326–333, 2007.

[16] J. Cavanagh, M. Cohen, and J. Allen, "Prelude to and resolution of an error: EEG phase synchrony reveals cognitive control dynamics during action monitoring," *The Journal of Neuroscience*, vol. 29, no. 1, pp. 98–105, 2009.

[17] J. Kayser and C. Tenke, "Principal components analysis of laplacian waveforms as a generic method for identifying ERP generator patterns: I. evaluation with auditory oddball tasks," *Clinical Neurophysiology*, vol. 117, no. 2, pp. 348–368, 2006.